

Pyrolysis of the Simplest Carbohydrate, Glycolaldehyde (CHO–CH₂OH), and Glyoxal in a Heated Microreactor

Jessica P. Porterfield,[†] Joshua H. Baraban,[†] Tyler P. Troy,[‡] Musahid Ahmed,[‡] Michael C. McCarthy,[§] Kathleen M. Morgan,^{||} John W. Daily,[⊥] Thanh Lam Nguyen,[#] John F. Stanton,[#] and G. Barney Ellison^{*,†}

[†]Department of Chemistry and Biochemistry and [⊥]Center for Combustion and Environmental Research, Department of Mechanical Engineering, University of Colorado, Boulder, Colorado 80309, United States

[‡]Chemical Sciences Division, Lawrence Berkeley National Laboratories, Berkeley, California 94720, United States

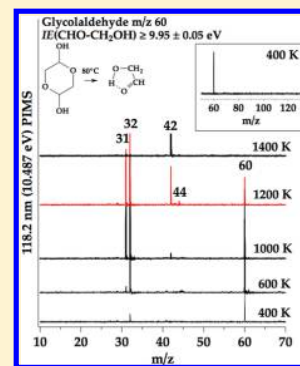
[§]Harvard-Smithsonian Center for Astrophysics, Cambridge, Massachusetts 02138, United States

^{||}Department of Chemistry, Xavier University of Louisiana, New Orleans, Louisiana 70125-1098, United States

[#]Department of Chemistry, University of Texas at Austin, Austin, Texas 78712, United States

Supporting Information

ABSTRACT: Both glycolaldehyde and glyoxal were pyrolyzed in a set of flash-pyrolysis microreactors. The pyrolysis products resulting from CHO–CH₂OH and HCO–CHO were detected and identified by vacuum ultraviolet (VUV) photoionization mass spectrometry. Complementary product identification was provided by argon matrix infrared absorption spectroscopy. Pyrolysis pressures in the microreactor were about 100 Torr, and contact times with the microreactors were roughly 100 μ s. At 1200 K, the products of glycolaldehyde pyrolysis are H atoms, CO, CH₂=O, CH₂=C=O, and HCO–CHO. Thermal decomposition of HCO–CHO was studied with pulsed 118.2 nm photoionization mass spectrometry and matrix infrared absorption. Under these conditions, glyoxal undergoes pyrolysis to H atoms and CO. Tunable VUV photoionization mass spectrometry provides a lower bound for the ionization energy (IE)(CHO–CH₂OH) $\geq 9.95 \pm 0.05$ eV. The gas-phase heat of formation of glycolaldehyde was established by a sequence of calorimetric experiments. The experimental result is $\Delta_f H_{298}(\text{CHO–CH}_2\text{OH}) = -75.8 \pm 1.3$ kcal mol⁻¹. Fully ab initio, coupled cluster calculations predict $\Delta_f H_0(\text{CHO–CH}_2\text{OH})$ of -73.1 ± 0.5 kcal mol⁻¹ and $\Delta_f H_{298}(\text{CHO–CH}_2\text{OH})$ of -76.1 ± 0.5 kcal mol⁻¹. The coupled-cluster singles doubles and noniterative triples correction calculations also lead to a revision of the geometry of CHO–CH₂OH. We find that the O–H bond length differs substantially from earlier experimental estimates, due to unusual zero-point contributions to the moments of inertia.



1. INTRODUCTION

Biomass is believed to be the only renewable source of carbon-based fuels and platform organic compounds.¹ In an effort to understand the mechanisms for the pyrolysis of biomass, we developed a heated microreactor for use as a flash pyrolysis flow reactor. Biofuel-related compounds mixed with helium or argon carrier gas are thermally decomposed in a resistively heated SiC microreactor (1 mm i.d. \times 2.5 cm length) at pressures of a few hundred Torr and temperatures of 1000–1600 K. Contact times with the microreactor are roughly 100 μ s. Decomposition products are detected by a combination of photoionization mass spectrometry (PIMS) and matrix infrared (IR) absorption spectroscopy.

The main components of biomass are carbohydrates and lignins. Carbohydrates are one of the most abundant classes of organic compounds on the planet.² To explore the pyrolysis mechanisms of carbohydrates, we intend to use dilute samples of sugars and use flash pyrolysis in a set of flow reactors. The simplest sugar is D-glyceraldehyde, CHO–CHOH–CH₂OH, and its Fischer projection is shown in Figure 1. Even this triose is complicated as the gas-phase heat of formation, bond

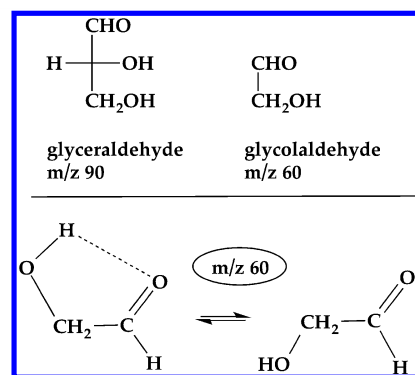


Figure 1. Chemical structures of glyceraldehyde and glycolaldehyde.

energies, precise molecular structure, and ionization energy are not known. A simpler molecule is glycolaldehyde (CHO–

Received: January 20, 2016

Revised: March 15, 2016

Published: March 16, 2016

CH₂OH) because it is the smallest possible hydroxyaldehyde. Glycolaldehyde is a carbohydrate, (C·H₂O)₂, and is the only possible diose. Even though it is not a true sugar, it must be understood first before the thermal decomposition of proper sugars can be tackled. Figure 1 relates glycolaldehyde to glyceraldehyde.

Surprisingly, the carbohydrate glycolaldehyde is an atmospherically relevant species.^{3,4} It is formed by the photo-oxidation^{5,6} of CH₂=CH₂ and is produced by forest fires.⁷ Oxidation⁸ of the volatile organic compound (VOC) 2-methyl-3-buten-2-ol (CH₂=CH-C(CH₃)₂OH) in an environmental chamber by OH in 700 Torr air degrades 50% of the VOC to CHO-CH₂OH. One of the most important of all VOCs is isoprene,^{9,10} and a major product of the photo-oxidation of CH₂=C(CH₃)-CH=CH₂ is methyl vinyl ketone (CH₃COCH=CH₂ or MVK). Further oxidation of MVK by OH radicals¹¹ leads to production of CHO-CH₂OH. Glycolaldehyde itself has been observed as a product of the fast pyrolysis of lignins; see Table 9 of ref 12. Its OH-initiated oxidation has been studied before,¹³ but to our knowledge this is the first gas-phase study of glycolaldehyde pyrolysis.

A product of the thermal cracking of glycolaldehyde is glyoxal (see Scheme 2), HCO-CHO. Both glyoxal and methylglyoxal (CH₃CO-CHO) are found in the atmosphere due to oxidation of biogenic compounds such as isoprene, oxidation of anthropogenic compounds (toluene, xylenes, and acetylene), and from combustion sources.^{14,15} Glyoxal and methylglyoxal can be taken up by atmospheric aerosols and have been shown to participate in secondary organic aerosol formation on aqueous aerosol particles and in clouds.^{16–19}

In this paper, we characterize the properties of CHO-CH₂OH and examine pathways for the pyrolysis of glycolaldehyde and glyoxal. We coupled reaction calorimetry with other experimental data to measure the gas-phase heat of formation of glycolaldehyde, Δ_fH₂₉₈(CHO-CH₂OH). We also performed ab initio electronic structure calculations to predict Δ_fH₂₉₈(CHO-CH₂OH) following a modified HEAT protocol.²⁰ Using coupled-cluster singles doubles and non-iterative triples correction (CCSD(T)) ab initio electronic structure calculations, we reanalyzed the existing microwave data and refined the molecular structure for glycolaldehyde by correcting the experimental rotational constants for zero-point vibrational motion. Ab initio methods were also used to predict the vibrational frequencies for glycolaldehyde and the ionization energy (IE)(CHO-CH₂OH). Tunable synchrotron vacuum ultraviolet (VUV) PIMS was used to measure the ionization threshold for glycolaldehyde and thus place a lower bound on the IE(CHO-CH₂OH). With the molecular structure, energetics, and IE of glycolaldehyde in hand, we performed the pyrolysis of CHO-CH₂OH in a heated microreactor. The pyrolysis of glyoxal has been carefully studied²¹ in a shock tube over the temperature range of 1100–2300 K while monitoring HCO (frequency modulation spectroscopy), HCO-CHO (UV absorption), and H atom (atom resonance absorption spectroscopy). We studied the thermal fragmentation of HCO-CHO in our microreactor as well, since glyoxal is a pyrolysis product of glycolaldehyde.

2. EXPERIMENTAL METHODS

2.1. Pyrolysis in a Microreactor. Three unique flash pyrolysis experiments were conducted for the study of glycolaldehyde: quasi-continuous PIMS with 500 MHz tunable photons, pulsed PIMS with 10 Hz fixed 10.487 eV photons, and

matrix-isolation IR spectroscopy. The microreactors have been described in detail elsewhere,^{22–25} but the following provides a brief description. The microreactors are resistively heated silicon carbide (SiC) tubes, which are either 2 or 3 cm long and 0.6 or 1 mm in diameter. Reactor wall temperatures are monitored by a Type C thermocouple (1.0% accuracy from 270 to 2300 K) that is fastened to the exterior of the tube with a 0.25 mm tantalum wire wrap. The heated region (distance between electrodes) is approximately 1–1.5 cm in length, and typical residence times are 25–150 μs.²⁶ Residence time is kept short intentionally to study the initial thermal products of unimolecular decomposition. Reaction chemistry is quenched when the gas mixture exiting the reactor expands supersonically into a vacuum chamber (1 × 10⁻⁷ to 1 × 10⁻⁶ Torr), thereby eliminating additional collisions. All stable, metastable, and radical intermediates and products are detected by PIMS and IR spectroscopy.

Glycolaldehyde is obtained as a solid dimer (see Figure 3). Low vapor pressure samples are introduced to the reactor by passing an inert carrier gas, helium or argon, through a temperature-controlled sample probe containing a few milligrams of reagent. Photoionization mass spectrometry is conducted at 10 Hz or 500 MHz allowing the sample probe temperature to be finely tuned (Love Controls Series 16A) to achieve a sufficient signal while simultaneously maintaining the low concentrations needed to establish unimolecular reaction conditions. Glycolaldehyde monomer was first observed at sample probe temperatures of about 80 °C, and no evidence for the gas-phase dimer was found. Glyoxal was first observed from the trimer dihydrate solid at sample probe temperatures of 120 °C.

At the University of Colorado, a solenoid pulsed valve supplies gas pulses to the sample probe and ultimately the reactor (3 cm length × 1 mm i.d.) at 10 Hz. Typical backing pressures are 1500 Torr, and at the exit of the reactor, a vacuum chamber is held at 1 × 10⁻⁶ Torr by a Varian VHS-6 diffusion pump (870 L sec⁻¹). The reactor exit faces a 2 mm i.d. skimmer less than 1 cm from the exit.²⁵ The skimmed molecular beam encounters fixed 118.2 nm (10.487 eV) photons supplied by the ninth harmonic of a Nd:YAG laser fired at 10 Hz. Dual-stage ion optics extract the resulting cations into a Jordan reflectron time-of-flight mass spectrometer equipped with chevron microchannel plate detectors. Typical mass resolution (Δ*m*/*m*) is 400, and spectra are averaged over 1000 scans.

The experiment conducted at LBNL's Advanced Light Source Beamline 9.0.2 is similar in principle to the experiment in Colorado. Continuous flow is used rather than pulsed, and 500 MHz tunable synchrotron radiation (7.4–19 eV) replaces a fixed VUV ionization source. Gas flow is maintained at 180 standard cm³ min⁻¹ (sccm) by an MKS P4B mass flow controller, and the reactor used at LBNL has subtly different dimensions (3 cm length × 0.6 mm i.d.). The continuous nature of the experiment increases signal by at least 2 orders of magnitude compared to the pulsed microreactor in Colorado. Typical backing pressures range from 100–300 Torr, depending upon reactor temperature, and pressure at the reactor exit is maintained just below 1 × 10⁻⁶ Torr. Typical photon fluxes²⁷ are roughly 1 × 10¹³ photons per second, and photoionization efficiency curves are normalized with respect to the photon flux at a given photon energy.

Matrix-isolation IR spectroscopy provides structural data as a complement to PIMS mass data. Argon carrier gas passes over the sample probe and is pulsed at approximately 10 Hz through

the reactor (2 mm length \times 1 mm i.d.), which is pointed at a cold CsI window. A two-stage helium cryostat (HC-2, APD Cryogenics) maintains the window at 20 K where argon deposits, thereby trapping the dilute products of decomposition. Backing pressure is about 800 Torr, and the exit pressure is maintained at 1×10^{-6} Torr by an Agilent TV 81 M turbo-pump. Infrared absorption spectra are collected with a Nicolet 6700 FT-IR equipped with a MCT-A detector (4000–650 cm^{-1}), and spectra are averaged over 500 scans with 0.25 cm^{-1} steps. Argon reaches notably lower temperatures than helium during the short residence times experienced in the reactor, and SiC wall temperatures must typically be 200 K higher to see similar results from the Colorado PIMS experiment.²⁶

2.2. Calorimetry. Materials. Anhydrous ethylene glycol (>99.5%) was used as purchased and was handled under argon. Solid glycolaldehyde dimer was recrystallized from boiling anhydrous methanol, under argon. The solution was cooled to room temperature and then crystallized over several weeks at 4 °C. The residual methanol was removed under vacuum, and the solid was stored in a desiccator.

The preweighed glass ampules for calorimetry runs²⁸ were first evacuated, heated to drive off moisture, then refilled with argon. Ethylene glycol was added by oven-dried, argon-flushed pipet, and the liquid was degassed before flame sealing under vacuum. The solid glycolaldehyde dimer was added to the ampule in an argon-filled glovebag and then sealed under vacuum. A microgram balance was used to obtain the sample mass to the nearest 0.000 001 g, reproducible to $\pm 0.000 005$ g.

Reaction Calorimetry. The custom reaction calorimetry system has been described previously^{29–31} and is a Wadsö-style submarine solution calorimeter.³² The argon-filled, airtight reaction vessel,³³ already containing the sealed ampule, was charged with roughly 150 mL of triethylene glycol dimethyl ether, dried using freshly activated alumina, and a solution of lithium triethyl borohydride in tetrahydrofuran³⁴ (1.0 M, 4.7 mL; 0.0047 mol, 0.5 g of LiEt_3BH).

The temperature is measured using a Hewlett-Packard quartz thermometer accurate to 0.0001 °C, calibrated against a water triple-point cell at 0 °C. For each reaction run, an electrical calibration is also performed. Each reaction was repeated multiple times to obtain the uncertainty in the measurement, which is reported as twice the standard deviation from the mean, as suggested by Rossini.³⁵

Differential Scanning Calorimetry. The enthalpy of fusion of glycolaldehyde dimer was obtained using the same recrystallized sample as was used for reaction calorimetry. The TA SDT Q600 DSC/TGA instrument was calibrated using an indium standard. The samples, in crimped aluminum pans, were heated from room temperature to 125 °C at a rate of 1 °C/min, with a flow rate of 50 mL/min. The sample mass was also recorded during the experiment and was shown to be constant.

2.3. Electronic Structure Calculations. The heat of formation of glycolaldehyde was calculated using a modified HEAT protocol.²⁰ Briefly, the molecular structure was optimized at the (all electron) AE-CCSD(T)/cc-pVQZ level of theory, followed by calculation of various electronic contributions to the energy. The core correlation contribution used here was [AE-CCSD(T)/cc-pCVQZ–FC-CCSD(T)/cc-pCVQZ], which reduces the uncertainty in the calculated heat of formation to 0.5 kcal mol^{-1} . Anharmonic zero-point energies (ZPE) were calculated at the (frozen core) FC-CCSD(T)/

ANO0 level of theory with ANO1 harmonic frequencies. We also performed a full FC-CCSD(T)/ANO1 anharmonic calculation and optimized an AE-CCSD(T)/cc-pCVQZ geometry in the course of the structure reinvestigation described below. The adiabatic ionization potentials of the two lowest states of the glycolaldehyde cation were calculated at the EOMIP-FC-CCSD/ANO1 level of theory, using ANO0 harmonic ZPEs. All calculations were performed using the CFOUR program system.³⁶

Calculations were also performed using CBS-APNO methodology,³⁷ as implemented in Gaussian 09W.³⁸ Structures were confirmed to be minima on the potential energy surface by verifying that the frequency calculation had no imaginary frequencies. If appropriate, exploration of molecular conformations was first done using lower-level theory in Spartan 08.³⁹

3. RESULTS

3.1. Molecular Structures. The CCSD(T) calculations predict the ground state of $\text{CHO}-\text{CH}_2\text{OH}$ to be the hydrogen-bonded cyclic structure in Figure 1. The open-chain conformations are all more than 3 kcal mol^{-1} higher in energy. The effective structure of glycolaldehyde has been determined previously by microwave spectroscopy.^{40,41} Figure 2 shows the

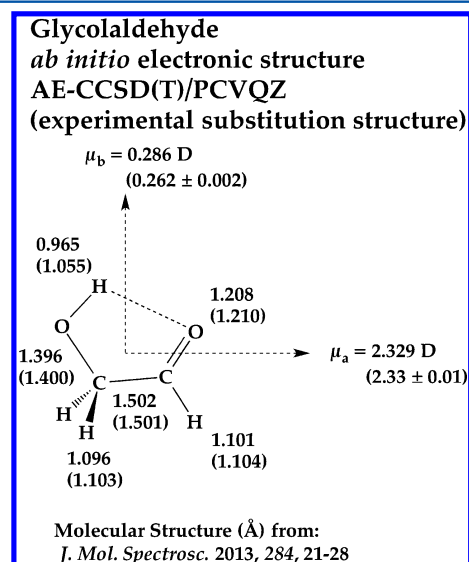


Figure 2. Molecular structures for \tilde{X}^1A' glycolaldehyde that result from CCSD(T) electronic structure calculations of the molecular geometry of $\text{CHO}-\text{CH}_2\text{OH}$. The values in parentheses are reported from earlier analysis of the microwave spectrum.⁴¹

results of CCSD(T) electronic structure calculations of the molecular geometry of $\text{CHO}-\text{CH}_2\text{OH}$; the electric dipole moments are in Debye and the experimental bond lengths (Å) are shown in parentheses.^{40,41} The purely *ab initio* structure is in good agreement with the microwave structure except for the OH bond length, which differs by approximately 0.1 Å, as noted by Carroll et al.⁴¹ Given the excellent agreement between our calculations and the measured rotational constants for all isotopes and the dipole moment, we reinvestigated the microwave structure determination using the published data^{41–44} and our calculated vibrational corrections to the rotational constants. We find that the large discrepancy in the OH bond length between the earlier experimental determinations and theory is due to unusual zero-point contributions

to the moments of inertia that are inferred from the rotational constants; when these are taken into account the discrepancy is largely (but not yet completely) resolved.

It is important to be precise in terminology when discussing molecular structures because several inequivalent types exist.⁴⁵ Generally speaking, structures are obtained from microwave data by relating moments of inertia that are inferred from the rotational constants to the atomic positions. The most conceptually straightforward procedure is to obtain data on isotopic species and solve a least-squares problem relating the inferred moments of inertia to a (unique) structure, which yields an effective r_0 structure. Unfortunately, r_0 structures make a number of assumptions—for one, that the geometry of isotopically substituted species are identical after vibrational effects are included—and so the ultimate goal is to determine the isotope-independent “vibrationless” r_e structure. The earlier experimental glycolaldehyde structures employed the “substitution method”,⁴⁶ where every atom is individually isotopically substituted to determine its position using the Kraitchman equations,^{47,48} which permits—again, subject to approximations—their Cartesian coordinates in the principal axis system to be obtained. As discussed by Costain,⁴⁶ the resulting r_s structure generally benefits from cancellation of zero-point vibrational effects and produces structures closer to r_e than the r_0 method, because usually $r_s \cong \frac{1}{2}(r_e + r_0)$.

However, the degree of agreement between r_s , r_e , and r_0 can vary, and the OH bond of glycolaldehyde appears to be a case where it does so significantly. The controlling factors in that relationship involve the ratios of the sum of the zero-point rotation–vibration corrections for each of the 18 fundamental modes ($\frac{1}{2}\sum\alpha$) and of the rotational constants between pairs of isotopes in the substitution method.^{45,46} These ratios are all contained within a range of about 15% for the single isotopic substitutions, except for the OH \rightarrow OD substitution where the zero-point rotation–vibration correction to the A rotational constant ($\frac{1}{2}\sum\alpha^A$) falls more than five times outside the usual variation. This extreme deviation appears to be caused primarily by α_1^A , the rotation–vibration correction associated with ν_1 , the OH stretch.

With the benefit of the ab initio vibrational corrections, we determine a semiexperimental r_e^{sc} structure by correcting the experimental rotational constants for zero-point vibration and performing a least-squares optimization of the 12 structural parameters. The OH bond length we obtain is 0.9528 ± 0.0005 Å, which while clearly in closer agreement with theory than the r_s value, still seems too short by roughly 0.01 Å. We also fit an r_0 structure where $R_{OH} = 1.041 \pm 0.006$ Å, in accordance with the previous r_s structures. We therefore conclude that zero-point vibrational effects are responsible for the previously noted discrepancy between theory and experiment (See the [Supporting Information](#) for details). Nevertheless, the unusual magnitude of the $r_0 - r_e$ shift and the short r_e OH bond length remain a curiosity, and further investigation is warranted.

3.2. Heat of Formation of Glycolaldehyde. The gas-phase heat of formation of glycolaldehyde, $\Delta_f H_{298}(\text{CHO}-\text{CH}_2\text{OH})$, was determined experimentally using a combination of thermochemical methods. To start, the condensed-phase heat of formation was obtained by reaction calorimetry. Combustion calorimetry has been used for carbohydrates in the past but with mixed results. For example, three combustion studies⁴⁹ on solid glycolaldehyde give combustion enthalpies over an unacceptably large range: -336.9 , -346.1 , and -348.9 kcal mol⁻¹, and this technique was not used in this study.

The condensed-phase structure of glycolaldehyde is complicated.⁵⁰ The solid form of glycolaldehyde is a dimer that can adopt two distinct conformations ([Figure 3](#)). Careful

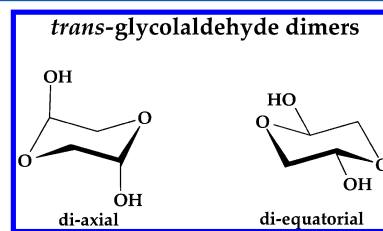
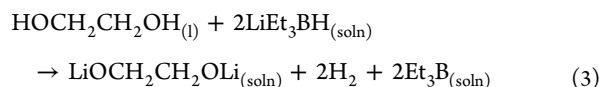
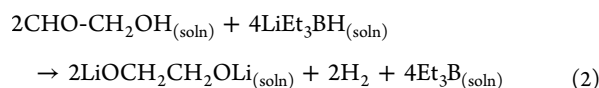


Figure 3. Structures of the *trans*-glycolaldehyde dimers.

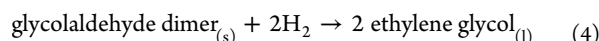
recrystallization can generate each structure separately.⁵¹ The X-ray crystal structure of the diaxial conformation has recently been reported.⁵² The solid dimer is thought to be stable indefinitely at room temperature.⁵¹ The melting point of the dimer is 80–90 °C, depending on the structure, and a viscous liquid persists for days at room temperature, which eventually solidifies. The liquid is composed of monomers, dimers, and potentially other structures such as oligomers,^{50,51} whose composition at room temperature presumably changes with time as crystallization occurs. As such, the stable and well-defined, solid dimeric form of glycolaldehyde was used for the reaction calorimetry experiments.

The heat of reduction (ΔH_{redn}) of pure, solid glycolaldehyde dimer to pure liquid ethylene glycol was obtained through a two-part thermochemical cycle. This reduction methodology has been successfully used to determine the gas-phase heat of formation for aldehydes and ketones,³⁴ esters,³⁵ and epoxides,³¹ with excellent agreement with existing experimental data and high-level calculations.^{31,54}

In the first reaction, the enthalpy change is measured for the process in which solid glycolaldehyde dimer is introduced to a solution of lithium triethylborohydride in triethylene glycol dimethyl ether, eventually affording the dianion of ethylene glycol in solution, $\Delta H(2)$. Note that the dimeric form of glycolaldehyde is in equilibrium with the monomer when dissolved in solution.⁵⁰ In the second reaction, the enthalpy change is measured for dissolving pure liquid $\text{HOCH}_2\text{CH}_2\text{OH}$ in the same reaction medium, yielding the same solution-phase dianion and hydrogen gas, $\Delta H(3)$. The uncertainty in these measurements is twice the standard deviation from the mean.³⁵



The enthalpies of reaction are measured to be $\Delta_{\text{rxn}}H(1 + 2) = -82.01 \pm 0.34$ kcal mol⁻¹ [for eqs 1 and 2] and $\Delta_{\text{rxn}}H(3) = -27.85 \pm 0.08$ kcal mol⁻¹. Combining reactions 1–3 gives



It is important to note that the solvated species that result from each of the two experiments are the same; hence, they

cancel. The difference is the heat of reduction of pure solid glycolaldehyde to pure liquid ethylene glycol:

$$\begin{aligned}\Delta H_{\text{redn}}(4) &= \Delta_{\text{rxn}}H(1 + 2) - 2\Delta_{\text{rxn}}H(3) \\ &= -26.32 \pm 0.36 \text{ kcal mol}^{-1}\end{aligned}\quad (5)$$

It is also true that the heat of reduction of the glycolaldehyde dimer is related to the heats of formation.

$$\begin{aligned}\Delta H_{\text{redn}}(4) &= 2\Delta_f H(\text{HOCH}_2\text{CH}_2\text{OH}, \text{l}) \\ &\quad - \Delta_f H(\text{glycolaldehyde dimer}, \text{s}) - 2\Delta_f H(\text{H}_2, \text{g})\end{aligned}\quad (6)$$

Ethylene glycol has been well-studied, and $\Delta_f H(\text{HOCH}_2\text{CH}_2\text{OH}, \text{l})$ has been determined by several research groups.⁴⁹ Using the value⁵⁵ of $-108.73 \pm 0.18 \text{ kcal mol}^{-1}$, the heat of formation of solid glycolaldehyde dimer is $-191.14 \pm 0.44 \text{ kcal mol}^{-1}$. The gas-phase heat of formation of glycolaldehyde is then determined by adding the heat of fusion (ΔH_{fus}) and the heat of vaporization (ΔH_{vap}). The ΔH_{fus} of the solid glycolaldehyde dimer was obtained by differential scanning calorimetry. Solid from the same recrystallized sample was used for this experiment as for the reaction calorimetry, so that the ratio of the dimeric conformers was constant. It was important to use a slow heating rate, $1 \text{ }^\circ\text{C}/\text{min}$, because the endothermic melting process was followed by a weak exotherm attributed to the dissociation of liquid dimer to liquid monomer. At this scan rate, the exothermic event was complete before sample evaporation occurred, and the final sample mass was $>99.5\%$ of the original mass as determined by thermogravimetric analysis. It is also important to note that there were no solid–solid transitions observed between room temperature and the observed fusion. The standard deviation of the three measurements is $0.2 \text{ kcal mol}^{-1}$. The ΔH_{fus} in (7) depends on a calibration constant determined by melting a reference compound, (in this case indium metal), and primarily because of this, the uncertainty of the measurement is increased to $0.4 \text{ kcal mol}^{-1}$, $\Delta H_{\text{fus, uncorrected}}(7) = 6.6 \pm 0.4 \text{ kcal mol}^{-1}$.



A temperature correction to 298.15 K should be applied to this ΔH_{fus} , which is valid at the midpoint of the melting range, approximately $85 \text{ }^\circ\text{C}$. The correction was made using the molar heat capacities of the solid and liquid; this correction was especially important to consider in this case because the structures of the solid dimer and liquid monomer are so different.

$$\Delta H_{\text{fus}, 298.15} = \Delta H_{\text{fus, uncorrected}} + (298.15 - T_{\text{mid}})(2C_{\text{pl}} - C_{\text{sl}})\quad (8)$$

The heat capacities were obtained by group additivity. For the liquid monomer, the Chueh–Swanson values were used,⁵⁶ giving $30.62 \text{ cal mol}^{-1} \text{ K}^{-1}$. For the solid dimer, the values tabulated by Acree and Chickos were used,⁵⁷ giving $33.2 \text{ cal mol}^{-1} \text{ K}^{-1}$. The temperature correction is $-1.7 \pm 0.3 \text{ kcal mol}^{-1}$, so the corrected $\Delta H_{\text{fus}, 298.15}(7)$ is $4.9 \pm 0.5 \text{ kcal mol}^{-1}$. The heat of formation of two moles of liquid glycolaldehyde is then $-186.2 \pm 0.7 \text{ kcal mol}^{-1}$, or $\Delta_f H_{\text{liq}}(\text{CHO-CH}_2\text{OH})$ is $-93.1 \pm 0.4 \text{ kcal mol}^{-1}$.

The ΔH_{vap} of glycolaldehyde can be calculated from vapor pressure versus temperature data available in the literature.⁵⁸ The linear data ($r^2 > 0.999$) were fit to the Clausius–Clapeyron equation and provide $\Delta H_{\text{vap}} = 16.9 \text{ kcal mol}^{-1}$ at 325.9 K. This value can be corrected to 298.15 K using heat capacities, obtained as described above for the liquid phase and using the

CBS-APNO calculated value of $15.6 \text{ cal mol}^{-1} \text{ K}^{-1}$ for the vapor phase. The corrected ΔH_{vap} is $17.3 \pm 1.2 \text{ kcal mol}^{-1}$; the uncertainty here is the same as in the literature data analysis. Together, these data lead to an experimental value for the gas-phase heat of formation for glycolaldehyde, $\Delta_f H_{298}(\text{CHO-CH}_2\text{OH})$, of $-75.8 \pm 1.3 \text{ kcal mol}^{-1}$.

The gas-phase ΔH_{redn} of glycolaldehyde to ethylene glycol can also be extracted from the $\Delta_f H_{298}(\text{CHO-CH}_2\text{OH})$ above and the $\Delta_f H_{\text{liq}}(\text{HOCH}_2\text{CH}_2\text{OH})$. The ΔH_{vap} for ethylene glycol $15.6 \pm 1.0 \text{ kcal mol}^{-1}$ (obtained as described for glycolaldehyde) is added to the $\Delta_f H_{\text{liq}}$ noted above. This gives the gas-phase $\Delta_f H_{298}(\text{HOCH}_2\text{CH}_2\text{OH})$ of $-93.1 \pm 1.0 \text{ kcal mol}^{-1}$ (which is in excellent agreement with Pedley et al.⁵⁹). The resulting $\Delta_{\text{redn}} H_{298}(\text{glycolaldehyde})$ is $-17.3 \pm 1.6 \text{ kcal mol}^{-1}$ and compares quite favorably to the $\Delta_{\text{redn}} H_{298}(\text{glycolaldehyde})$ value, calculated using CBS-APNO methodology,³⁷ of $-17.1 \text{ kcal mol}^{-1}$. In the CBS-APNO calculations, three conformations of $\text{CHO-CH}_2\text{OH}$ and 10 conformations of $\text{HOCH}_2\text{CH}_2\text{OH}$ were considered⁶⁰ with appropriate multiplicity in an energy-weighted average. The correction to ethylene glycol due to the higher-energy conformations amounts to $0.2 \text{ kcal mol}^{-1}$ (See the [Supporting Information](#) for further details.)

There have been earlier attempts^{61,62} to use electronic structure calculations to predict the gas-phase heat of formation of glycolaldehyde. A G2 calculation reported $\Delta_f H_{298}(\text{CHO-CH}_2\text{OH})$ to be $-77.6 \pm 1.2 \text{ kcal mol}^{-1}$, while the G3/DFT prediction was $-75.6 \pm 0.8 \text{ kcal mol}^{-1}$. We performed a fully ab initio calculation of the gas-phase heat of formation of glycolaldehyde. We applied the modified HEAT protocol²⁰ (described above) and found $\Delta_f H_0(\text{CHO-CH}_2\text{OH}) = -73.1 \pm 0.5 \text{ kcal mol}^{-1}$ and $\Delta_f H_{298}(\text{CHO-CH}_2\text{OH}) = -76.1 \pm 0.5 \text{ kcal mol}^{-1}$. There is good agreement between this completely ab initio heat of formation ($-76.1 \pm 0.5 \text{ kcal mol}^{-1}$) and the calorimetrically measured result ($-75.8 \pm 1.3 \text{ kcal mol}^{-1}$).

Although the CBS-APNO method is a composite method and is “slightly empirical,” we also used this procedure to estimate the heat of formation of glycolaldehyde. Using the CBS-APNO methodology,^{37,38} the reduction to ethylene glycol was calculated.



The $\Delta_{\text{rxn}} H_{298}(9)$ was calculated to be $-17.1 \text{ kcal mol}^{-1}$. Since the experimentally determined⁵⁵ $\Delta_f H_{298}(\text{HOCH}_2\text{CH}_2\text{OH})$ is $-93.1 \pm 1.0 \text{ kcal mol}^{-1}$, the $\Delta_f H_{298}(\text{glycolaldehyde})$ calculated by the CBS-APNO method is $-76 \pm 1 \text{ kcal mol}^{-1}$.

3.3. Ionization Energy of Glycolaldehyde. The ionization potential for glycolaldehyde has been measured⁶³ by threshold electron impact ionization to be $\text{IE}(\text{CHO-CH}_2\text{OH}) \geq 10.2 \pm 0.1 \text{ eV}$. To confirm this value, we used tunable VUV radiation to study the photoionization of glycolaldehyde. [Figure 4](#) shows the photoionization efficiency curve, $\text{PIE}(m/z 60)$, that results from glycolaldehyde ($\text{CHO-CH}_2\text{OH}$), at 400 K in a continuous He microreactor. The appearance energy for $\text{CHO-CH}_2\text{OH}^+$ ($m/z 60$) fixes a lower bound on the ionization energy of $\text{IE}(\text{CHO-CH}_2\text{OH}) \geq 9.95 \pm 0.05 \text{ eV}$. This is slightly below the electron impact result⁶³ of $10.2 \pm 0.1 \text{ eV}$.

The electronic states of the $\text{CHO-CH}_2\text{OH}^+$ ion can be understood with the generalized valence bond diagrams⁶⁴ in [Scheme 1](#). Ionization at the carbonyl group produces a ${}^2A'$ ion that relaxes to the nonplanar $\tilde{X}^+ {}^2A^+$ cation. Photoionization of the alcohol yields the $\tilde{A}^+ {}^2A^+$ excited state that is expected to be

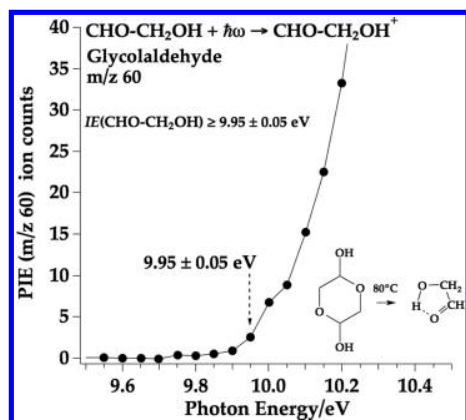


Figure 4. Photoionization efficiency scan for the parent ion m/z 60 resulting from heating glycolaldehyde in a continuous-flow He microreactor at Beamline 9.0.2 at the Advanced Light Source.

about 0.5 eV above the ground state. The ab initio calculated ionization gives $IE(\text{CHO}-\text{CH}_2\text{OH}) = 10.0 \pm 0.2$ eV and is consistent with the experimental spectrum in Figure 4. The ground state of the $\text{CHO}-\text{CH}_2\text{OH}^+$ is found to be the nonsymmetric $\tilde{X}^+ 2A$ state. The excited state, $\tilde{A}^+ 2A''$ ($\text{CHO}-\text{CH}_2\text{OH}^+$), is calculated to be 0.2 eV higher than the \tilde{X}^+ state.

3.4. Pyrolysis of Glycolaldehyde and Glyoxal. The pyrolysis pathways for $\text{CHO}-\text{CH}_2\text{OH}$ can be evaluated by use of the known⁶⁵ heats of formation of the radicals and the measured $\Delta_f H_{298}(\text{CHO}-\text{CH}_2\text{OH})$. Most of the relevant energetics for thermal cleavage of glycolaldehyde are shown in Table 1. Scheme 2 shows the likely pathways for thermal dissociation of glycolaldehyde. Cleavage of the C–C bond, $\text{CHO}-\text{CH}_2\text{OH}$, requires 82 kcal mol^{-1} and produces the reactive radicals HCO and CH_2OH . In the hot microreactor,

Table 1

experimental thermochemistry, kcal mol^{-1}			
(1)	$\Delta H_{298}(\text{CH}_3-\text{CH}_3)$	90.2 ± 0.1	59,65
(2)	$\Delta H_{298}(\text{CH}_3-\text{CHO})$	84.8 ± 0.2	59,65
(3)	$\Delta H_{298}(\text{CH}_3-\text{CH}_2\text{OH})$	87.2 ± 0.2	59,65
(4)	$\Delta H_{298}(\text{trans HCO}-\text{CHO})$	70.8 ± 0.3	59,65,79,80
(5)	$\Delta H_{298}(\text{CHO}-\text{CH}_2\text{OH})$	82 ± 1	this work
(6)	$\Delta H_{298}(\text{H}-\text{CH}_2\text{CH}_3)$	101.1 ± 0.4	59,65
(7)	$\Delta H_{298}(\text{H}-\text{CH}_2\text{OH})$	96.1 ± 0.2	59,65
(8)	$\Delta H_{298}(\text{CH}_3\text{CO}-\text{H})$	89.3 ± 0.4	59,65
(9)	$\Delta H_{298}(\text{H}-\text{CH}_2\text{CHO})$	94 ± 2	59,65
(10)	$\Delta H_{298}(\text{CH}_3-\text{CO})$	11.1 ± 0.4	59,65
(11)	$\Delta H_{298}(\text{H}-\text{CO})$	15.6 ± 0.1	59,65
(12)	$\Delta H_{298}(\text{CH}_2\text{O}-\text{H})$	30.2 ± 0.2	59,65
ionization energies, eV			
m/z	species	ionization energy	
1	H	13.59844 ± 0.00001	81
17	OH	13.01698 ± 0.00025	82
28	CO	14.0136 ± 0.0005	83
30	$\text{CH}_2=\text{O}$	10.8850 ± 0.0002	84
32	O_2	12.0696 ± 0.0002	85
42	$\text{CH}_2=\text{C}=\text{O}$	9.6191 ± 0.0004	86
44	$\text{CH}_2=\text{CHOH}$	$\geq 9.33 \pm 0.05$	87
44	CH_3CHO	10.2295 ± 0.0007	88
58	HCO–CHO	10.2 ± 0.1	76
60	$\text{CHO}-\text{CH}_2\text{OH}$	$\geq 9.95 \pm 0.05$	this work

these radicals will rapidly decompose to H atoms, CO, and $\text{CH}_2=\text{O}$. We estimate that rupture of the $\text{HOCH}_2\text{CO}-\text{H}$ bond will require⁶⁵ roughly 88 kcal mol^{-1} and furnishes the acyl radical, $\text{HOCH}_2\text{CO}^\bullet$, and H atoms. Rapid decomposition of the acyl radical yields (OH and $\text{CH}_2=\text{C}=\text{O}$) or (CO and CH_2OH). Finally, cleavage of the methylene C–H bond of glycolaldehyde generates H atom and the HOCHCHO radical. Thermal cracking of the HOCHCHO radical makes H atoms and glyoxal, HCO–CHO. It is also possible that glycolaldehyde could isomerize to the enediol ($\text{HOCH}=\text{CHOH}$), and concerted reaction mechanisms, such as loss of water to form ketene, are also possible.

The unimolecular fragmentation pathways in Scheme 2 all produce H atoms. It is known⁶⁶ that hydrogen atoms are very reactive in these hot microreactors. Scheme 3 shows the likely products that result from H atom chemistry with glycolaldehyde. The H atoms could add to the carbonyl C atom to produce the $\text{HOCH}_2\text{CH}_2\text{O}$ radical. This alkoxy radical is expected to rapidly fragment to CH_2OH and $\text{CH}_2=\text{O}$. Alternatively H atoms could add to the carbonyl O atom and generate the HOCH_2CHOH radical. Loss of OH leads to the enol, $\text{CH}_2=\text{CHOH}$. Isomerization of the enol produces CH_3CHO , which fragments^{22,27} in the hot microreactor.

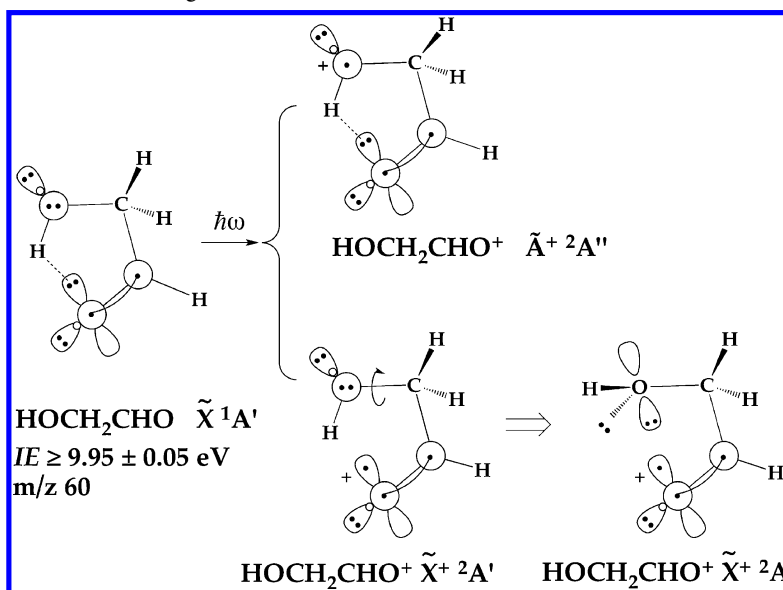
A good strategy to avoid the H atom chemistry sketched in Scheme 3 would be to perform the pyrolysis of $\text{CHO}-\text{CH}_2\text{OH}$ under conditions of high dilution. Commonly, dilution of the fuel to approximately 0.1% or less in the He carrier gas leads to suppression of bimolecular chemistry. This is not so easy to accomplish with glycolaldehyde, because the starting material is not $\text{CHO}-\text{CH}_2\text{OH}$ but the solid dimer.

Figure 5 shows the 118.2 nm (10.487 eV) PIMS that results when glycolaldehyde is heated to 1400 K. The bottom scan is from a sample of the glycolaldehyde dimer heated to 80 °C. The inset at the top reveals that there are no signals from the (dimer glycolaldehyde)⁺ at m/z 120, which implies that this species does not survive in the beam. The spectrum shows an intense peak at m/z 60 that is assigned to $\text{CHO}-\text{CH}_2\text{OH}^+$; this is consistent with the ionization threshold of 9.95 ± 0.05 in Figure 4. The presence of the feature at m/z 32 demonstrates that $\text{CHO}-\text{CH}_2\text{OH}$ is subject to dissociative ionization.

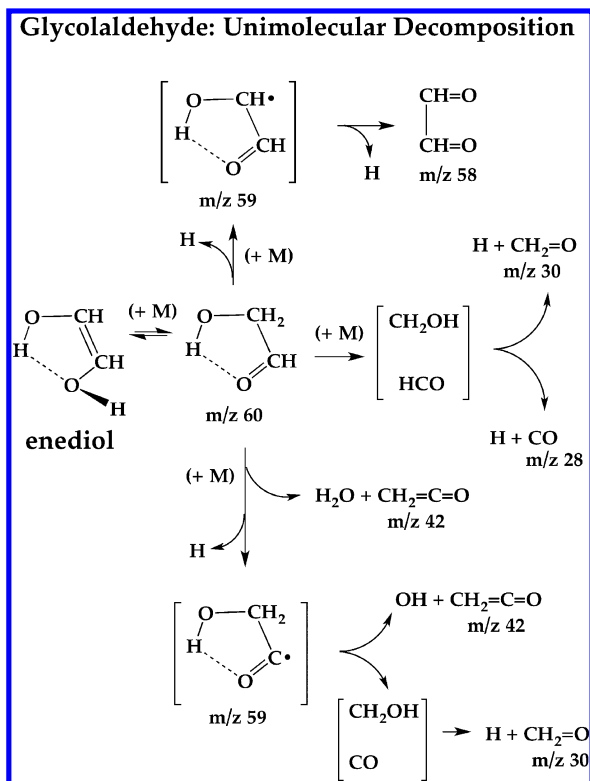


Scheme 4 suggests dissociation pathways for the glycolaldehyde cation. The ground $\tilde{X}^+ 2A$ state of the $\text{CHO}-\text{CH}_2\text{OH}^+$ cation is subject to β -scission that could produce either the stable ions HCO⁺ (m/z 29) or $\text{CH}_2=\text{OH}^+$ (m/z 31). Ionization of the alcohol produces the excited state $\tilde{A}^+ 2A''$, which could internally abstract at the acyl group and generate the metastable $[\text{H}_2\text{O}-\text{CH}_2-\text{CO}^\bullet]^+$ distonic ion. Loss of water leads to the ketene radical-cation, CH_2CO^+ (m/z 42), or loss of CO generates the $[\text{H}_2\text{O}-\text{CH}_2^\bullet]^+$ (m/z 32) distonic cation. (In an earlier photoionization study,⁶⁷ dissociative ionization of glycolaldehyde with loss of CO to produce m/z 32 was observed.) Because the splitting between the $\tilde{X}^+ 2A$ and $\tilde{A}^+ 2A''$ states of the $\text{CHO}-\text{CH}_2\text{OH}^+$ is about 240 meV (see Section 3.3), the 118.2 nm (10.487 eV) ionizing laser will produce both low-lying states of the $\text{CHO}-\text{CH}_2\text{OH}^+$ cation. On the basis of these energetics and Scheme 4, we assign the dissociative ion m/z 32 in Figure 5 to be the $[\text{H}_2\text{O}-\text{CH}_2^\bullet]^+$ distonic cation.

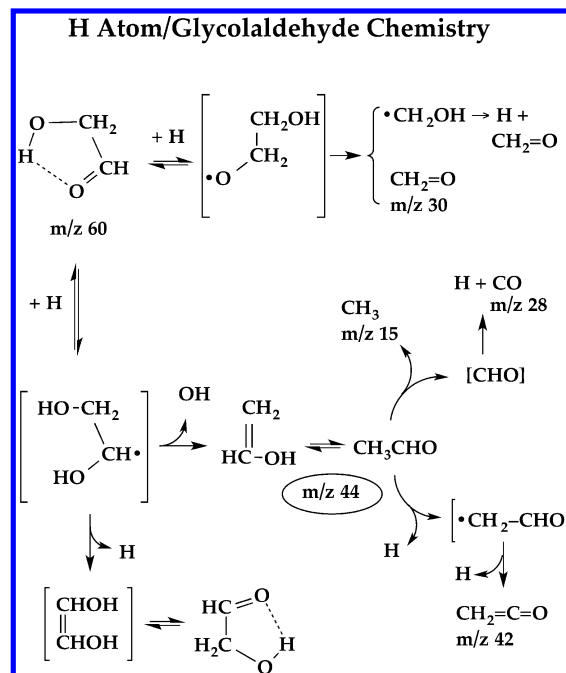
As the microreactor is heated to 600 K a peak at m/z 31 appears (Figure 5). A possible explanation could be isomerization of $\text{CHO}-\text{CH}_2\text{OH}$ to the enediol, $\text{HOCH}=\text{CHOH}$. Ionization energies of enols are roughly 1 eV below the keto

Scheme 1. Generalized Valence Bond Diagrams for the Ground and Excited States of the CHO-CH₂OH⁺ Cation

Scheme 2



Scheme 3



tautomer, so $IE(\text{HOCH}=\text{CHOH})$ is probably approximately 9 eV. Photoionization of the enediol produces the $[\text{HOCH}=\text{CHOH}]^+$ cation, which is subject to rearrangement⁶⁸ to the $\tilde{X}^+ 2A$ $[\text{CHO}-\text{CH}_2\text{OH}]^+$ ion that is chemically activated by about 1.5 eV. In Figure 5 we assign the feature at $m/z \ 31$ to the $\text{CH}_2=\text{OH}^+$ ion. As the reactor is heated to 1000 K, a peak at $m/z \ 42$ is observed and is assigned to CH_2CO^+ . This could be due to dissociative ionization of the enediol or ketene as a thermal product. At 1200 K, $m/z \ 42$ becomes much more intense.

It is difficult to say if there is any H atom chemistry as described in Scheme 3. Addition of H atoms to O atoms could lead to production of OH radicals and the enol, $\text{CH}_2=\text{CHOH}$. There are weak signals at $m/z \ 44$ when $\text{CHO}-\text{CH}_2\text{OH}$ is heated to 1200 K. These signals probably arise from small amounts of $\text{CH}_2=\text{CHOH}$ but are unlikely to originate from CH_3CHO . Acetaldehyde is known^{22,27} to thermally dissociate to CH_3 and HCO radicals, but no methyl radicals ($m/z \ 15$) are ever detected. Any hydroxyl radicals that result from the H atom chemistry in Scheme 3 would form water by reaction with parent glycolaldehyde.⁶⁹

One way to avoid the confusing PIMS signals that result from dissociative ionization is to use IR spectroscopy as a diagnostic of the pyrolysis products. The IR spectrum of

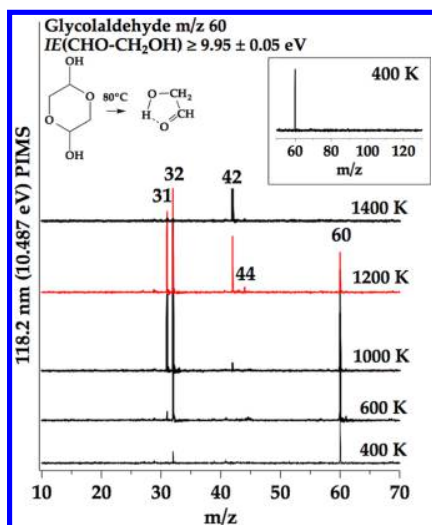
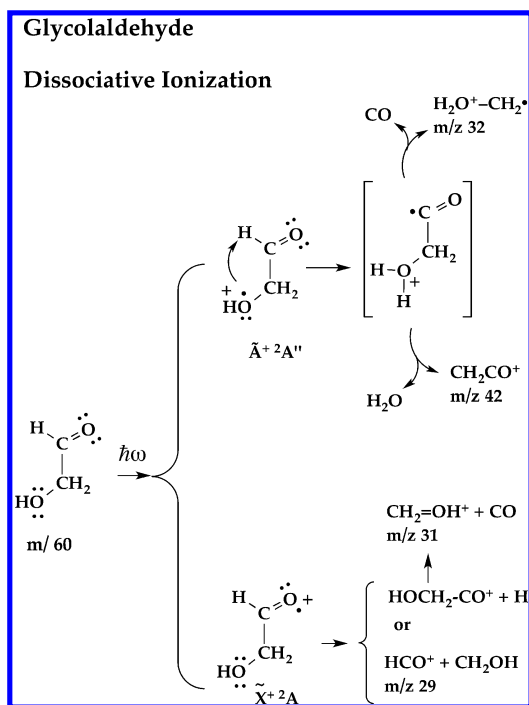


Figure 5. 118.2 nm VUV PIMS scans resulting from heating glycolaldehyde in a pulsed He microreactor.

Scheme 4



CHO-CH₂OH has been studied in the gas phase⁵⁰ and in matrices.⁷⁰ We performed CCSD(T)/VPT2 calculations for the fundamental vibrational modes of glycolaldehyde. Table 2 compares the ab initio frequencies with the experimental findings^{50,70} and the transitions observed in an Ar matrix.

Figure 6 shows the IR spectrum that results when glycolaldehyde is heated to 1500 K. The presence of formaldehyde is clearly demonstrated^{71,72} by observation of $\nu_1(\text{CH}_2=\text{O})$, $\nu_2(\text{CH}_2=\text{O})$, and $\nu_3(\text{CH}_2=\text{O})$. Glyoxal⁷³ is identified as a thermal product by observation of $\nu_{10}(\text{HCO-CHO})$. Scheme 2 has a possible path for glyoxal formation; however, the thermochemistry in Table 1 shows $\Delta_f H_{298}(\text{HCO-CHO})$ to be 71 kcal mol⁻¹. Because of the relatively low HCO-CHO bond energy, we expect (Table 1) that most

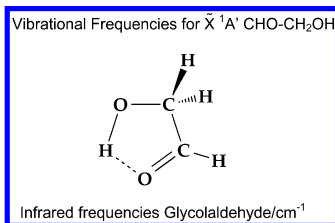
glyoxal will dissociate to a pair of HCO radicals, which in turn fragment to H atoms and CO. Additional concerted reactions have been shown to predominate at lower temperatures;²¹ however, little evidence is seen of this under our conditions at 1500 K in the Fourier transform IR. There is a new >C=O band appearing to the blue of $\nu_4(\text{CHO-CH}_2\text{OH})$, which is assigned to an open-chain conformer of glycolaldehyde in Figure 1. An additional peak at 1737 cm⁻¹ is observed and attributed to ν_2 of the (CH₂=O, H₂O) dimer.⁷⁴ The unassigned peak at 1767 cm⁻¹ observed at 300 and 1500 K is perhaps due to a similar interaction between water and glycolaldehyde. Additionally, Figure 7 establishes the presence of ketene⁷⁵ as a thermal product with detection of $\nu_7(\text{CH}_2=\text{C}=\text{O})$, $\nu_2(\text{CH}_2=\text{C}=\text{O})$, and $\nu_3(\text{CH}_2=\text{C}=\text{O})$.

To confirm the pyrolysis of glyoxal HCO-CHO (+ M) → [HCO + HCO] → 2 H + 2 CO, an authentic sample of HCO-CHO was decomposed in a hot SiC reactor (see Figure 6). The IE(HCO-CHO) is reported⁷⁶ to be 10.2 eV (Table 1). Figure 8 shows the PIMS of a dilute mixture of glyoxal in He is vaporized in a microreactor at 120 °C (400 K), and the parent peak (*m/z* 58) is the dominant feature in the spectrum. As the reactor is heated to 1200 K, the [HCO-CHO]⁺ *m/z* 58 signal begins to drop. By 1400 K in He, all signals fade from the 118.2 nm PIMS spectrum, because the pyrolysis products of glyoxal, H, and CO in eq 10, cannot be photoionized by 10.487 eV radiation (see Table 1). Figure 9 shows the IR spectra that result from heating glyoxal in Ar.^{73,77} By 1500 K, the HCO-CHO is largely destroyed, and intense signals of CO are observed. Figure 9 shows the appearance of clusters of carbon monoxide⁷⁸ that result from the pyrolysis of glyoxal. We do not observe any formaldehyde that would arise from the previously observed glyoxal molecular decomposition channels.²¹

4. CONCLUSIONS

Dilute samples of both glycolaldehyde and glyoxal have been subjected to flash pyrolysis in a heated microreactor. Pyrolysis of CHO-CH₂OH produces H atoms, formaldehyde, glyoxal, and carbon monoxide. The unimolecular chemistry in Scheme 2 can account for all of these products. The intense IR signals for CH₂=O are consistent with cleavage of the C-C bond making the HCO and CH₂OH radicals that produce H, CO, and CH₂=O. Cleavage of the C-H methylene bond in glycolaldehyde leads to the formation of HCO-CHO and H atoms. Thermal cracking of glycolaldehyde to produce H atoms and •CO-CH₂OH radicals generates CH₂=O as well as ketene, CH₂=C=O. The fate of glyoxal is simple. Pyrolysis of HCO-CHO under our conditions produces a pair of formyl radicals that decompose to H atoms and CO.

Because the molecular properties of glycolaldehyde are not well-established, we have measured both the gas-phase heat of formation and ionization threshold for CHO-CH₂OH. The $\Delta_f H_{298}(\text{CHO-CH}_2\text{OH})$ has been determined by a combination of calorimetric measurements and ab initio electronic structure calculations. Calorimetric studies of the heat of reduction of glycolaldehyde in solution lead to a determination of the heat of formation of solid glycolaldehyde dimer to be -191.1 ± 0.4 kcal mol⁻¹. Measurement of ΔH_{fusion} and ΔH_{vap} results in a value of the gas-phase heat of formation for glycolaldehyde, $\Delta_f H_{298}(\text{CHO-CH}_2\text{OH})$, as -75.8 ± 1.3 kcal mol⁻¹. Electronic structure calculations predict values for the heat of formation of glycolaldehyde that agree well with the experimental determination. The $\Delta_f H_{298}(\text{glycolaldehyde})$ calculated by the CBS-APNO method is -76 ± 1 kcal mol⁻¹. More

Table 2. Vibrational Frequencies and Assignments^a for Glycolaldehyde

mode	CCSD(T)/VPT2	A, km mol ⁻¹	gas phase ⁵⁰	Ar matrix (this work, ±0.3 cm ⁻¹)	relative intensity	
A'	ν_1	3557	39	3585/3565/3546	3551/3543/3535	10/25/13
	ν_2	2923*	10	2920	2911/2906/2895	2/2/3
	ν_3	2813/2842*	33/11	2835/2810	2853/2846/2835	5/6/2
	ν_4	1751/1692*	83/11	1764/1753/1742	1767/1747/1697/1695	3/186/18/9
	ν_5	1454/1429*	7/16	1440/1468	1443/1429/1424	4/5/4
	ν_6	1404*	30	1410	1402	5
	ν_7	1366	14	1376/1359	1366/1365/1361	42/19/5
	ν_8	1284/1272*	11/21	1299/1282/1273/1268/1266/1258	1272/1268/1266	6/25/19
	ν_9	1112*	61	1117/1112/1110/1097	1131/1112/1110/1108	6/12/100/45
	ν_{10}	853	43	871/861/859/845	860/858/857/856/855	7/18/12/68/29
	ν_{11}	745	8	762/752/750/748/746/743/738	751/749	7/7
	ν_{12}	280	23			
A''	ν_{13}	2873*	25	2880	2880	1
	ν_{14}	1223*	2	1146	1251/1232/1228	2
	ν_{15}	1083	1	1070/1059/1050	1067	6
	ν_{16}	709	0			
	ν_{17}	340	83			
	ν_{18}	200	6			
$2\nu_7$	2715	3	2717/2696	2713/2711	5/3	
$\{\nu_{12}, \nu_{18}\} + \{\nu_{11}, \nu_{16}\}$			916	999/997/951/935	5/4/3/2	

^aThe VPT2 calculations use CCSD(T)/ANO0 anharmonic constants and CCSD(T)/ANO1 harmonic frequencies. Asterisks mark cases where resonances were treated by diagonalization. Potential combination/overtone bands for unidentified observed peaks have also been reported.

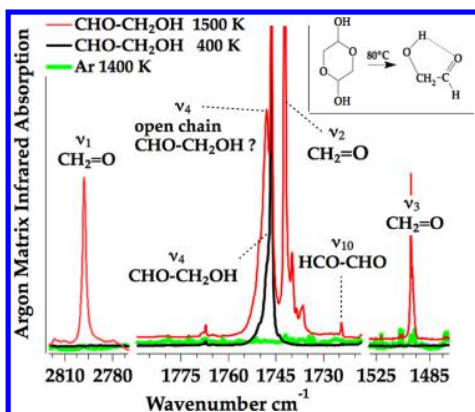


Figure 6. Matrix IR spectra that result from heating glycolaldehyde in a pulsed Ar microreactor. The black trace is the IR spectrum⁷⁰ of CHO-CH₂OH produced by heating glycolaldehyde dimer to 80 °C. The green trace is a background that results from heating Ar to 1500 K in the SiC microreactor. Both formaldehyde^{72,73} and glyoxal^{73,77} are present.

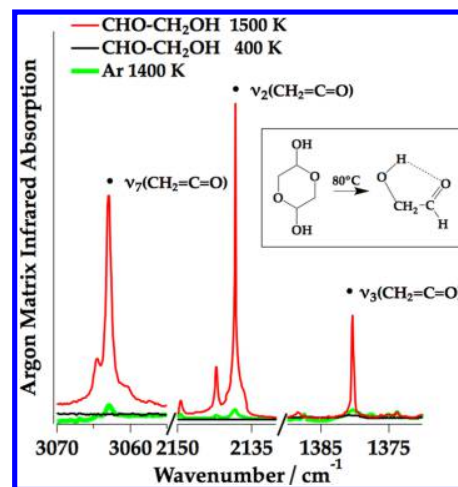


Figure 7. Matrix IR spectra that result from heating glycolaldehyde in a pulsed Ar microreactor. The black trace is the IR spectrum⁷⁰ of CHO-CH₂OH produced by heating glycolaldehyde dimer to 80 °C. The green trace is a background that results from heating Ar to 1500 K in the SiC microreactor. Ketene is clearly present.⁷⁵

precise, fully ab initio calculations using the modified HEAT protocol²⁰ predict $\Delta_f H_0(\text{CHO}-\text{CH}_2\text{OH})$ of -73.1 ± 0.5 kcal mol⁻¹ and $\Delta_f H_{298}(\text{CHO}-\text{CH}_2\text{OH})$ of -76.1 ± 0.5 kcal mol⁻¹. The electronic structure calculations, both CBS-APNO and modified HEAT, of the heat of formation for glycolaldehyde are in excellent agreement with the calorimetrically determined result of -75.8 ± 1.3 kcal mol⁻¹.

A lower bound to IE(CHO-CH₂OH) was fixed by the appearance energy of the [CHO-CH₂OH]⁺ with tunable synchrotron radiation, IE(CHO-CH₂OH) $\geq 9.95 \pm 0.05$ eV. This ionization threshold is consistent with ab initio electronic structure calculations. Coupled cluster calculations find the ionization energy of glycolaldehyde to be 10.0 ± 0.2 eV, in

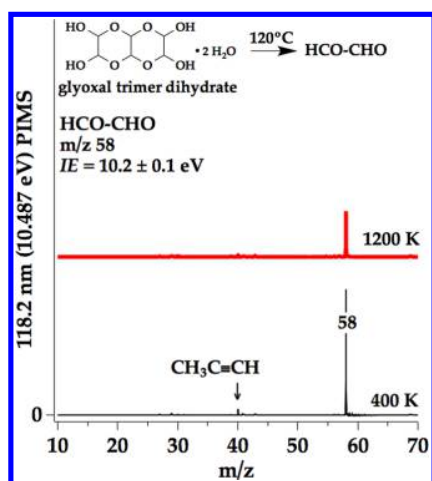


Figure 8. 118.2 nm VUV PIMS scans resulting from heating glyoxal in a pulsed He microreactor. The band at m/z 40 is a $\text{CH}_3\text{C}\equiv\text{CH}$ background contamination.

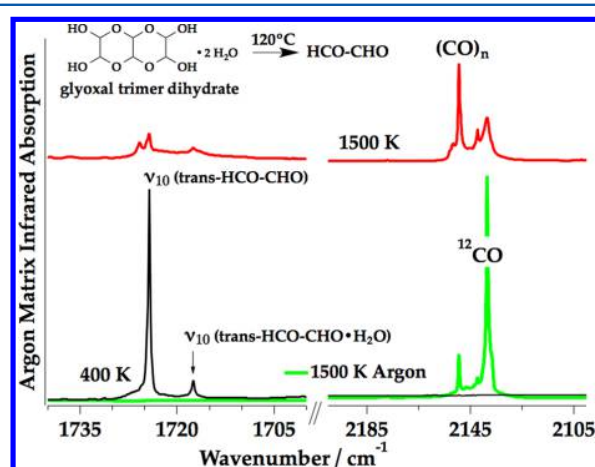


Figure 9. Matrix IR spectra that result from heating glyoxal trimer dihydrate in a pulsed Ar microreactor. The black trace is the IR spectrum^{73,77} of HCO-CHO produced by heating glyoxal to 120°C . The intense glyoxal fundamental ν_{10} is detected at 1724 cm^{-1} , and the (water, glyoxal) complex⁸⁹ is observed at 1717 cm^{-1} . The green trace is a background that results from heating Ar to 1500 K in the SiC microreactor.

agreement with the experimental bound. Coupled cluster calculations were also used to analyze the molecular structure of glycolaldehyde and to revise the geometry of this carbohydrate. We find that equilibrium O–H bond length is considerably shorter than suggested by experimental determinations of the effective r_0 structure on account of unusual zero-point contributions, primarily from the ν_1 OH stretch.

These successful efforts to understand the thermal cracking and the molecular properties of both glyoxal and glycolaldehyde encourage us to believe that the pyrolysis of complex sugars can be understood as well.

■ ASSOCIATED CONTENT

● Supporting Information

The Supporting Information is available free of charge on the ACS Publications website at DOI: 10.1021/acs.jpca.6b00652.

The Supporting Information contains (a) an analysis of the rotational spectra of glycolaldehyde and (b) details of

the reaction calorimetry, including differential scanning calorimetry results and heats of vaporization. (PDF)

■ AUTHOR INFORMATION

Corresponding Author

*E-mail: barney@jila.colorado.edu.

Notes

The authors declare no competing financial interest.

■ ACKNOWLEDGMENTS

The National Science Foundation (CBET-1403979) has provided support for J.P.P., J.H.B., J.W.D., and G.B.E. We would like to acknowledge National Science Foundation (CHE-1361874) to K.M.M. and CHE-1361031 to J.F.S. Thermal analysis measurements were performed with assistance from S. Akbarian-Tefaghi at the Univ. of New Orleans, Advanced Materials Research Institute FACS user facility. J.F.S. and T.L.N. acknowledge support from the Robert A. Welch Foundation (Grant No. F-1283) and the United States Department of Energy, Basic Energy Sciences (DE-FG02-07ER15884). M.A. and T.P.T. and the Advanced Light Source are supported by the Director, Office of Energy Research, Office of Basic Energy Sciences, and Chemical Sciences Division of the U.S. Department of Energy under Contract No. DE-AC02-05CH11231. We thank Prof. K. B. Wiberg for several helpful comments.

■ REFERENCES

- (1) Caes, B. R.; Palte, M. J.; Raines, R. T. Organocatalytic Conversion of Cellulose into a Platform Chemical. *Chem. Sci.* **2013**, *4*, 196–199.
- (2) Streitwieser, A.; Kosower, E. M.; Heathcock, C. H. *Introduction to Organic Chemistry*, 4th ed.; Prentice Hall: Upper Saddle River, NJ, 1977.
- (3) Bacher, C.; Tyndall, G. S.; Orlando, J. J. The Atmospheric Chemistry of Glycolaldehyde. *J. Atmos. Chem.* **2001**, *39*, 171–189.
- (4) Johnson, T. J.; Sams, R. L.; Profeta, L. T. M.; Akagi, S. K.; Burling, I. R.; Yokelson, R. J.; Williams, S. D. Quantitative IR Spectrum and Vibrational Assignments for Glycolaldehyde Vapor: Glycolaldehyde Measurements in Biomass Burning Plumes. *J. Phys. Chem. A* **2013**, *117*, 4096–4107.
- (5) Niki, H.; Maker, P. D.; Savage, C. M.; Breitenbach, L. P. An FTIR Study of Mechanisms for the OH Radical Initiated Oxidation of C_2H_4 in the Presence of NO - Detection of Glycolaldehyde. *Chem. Phys. Lett.* **1981**, *80*, 499–503.
- (6) Orlando, J. J.; Tyndall, G. S.; Bilde, M.; Ferronato, C.; Wallington, T. J.; Vereecken, L.; Peeters, J. Laboratory and Theoretical Study of the Oxy Radicals In The OH and Cl-Initiated Oxidation of Ethene. *J. Phys. Chem. A* **1998**, *102*, 8116–8123.
- (7) Yokelson, R. J.; Susott, R.; Ward, D. E.; Reardon, J.; Griffith, D. W. T. Emissions From Smoldering Combustion of Biomass Measured by Open-Path Fourier Transform Infrared Spectroscopy. *J. Geophys. Res. - Atm.* **1997**, *102*, 18865–18877.
- (8) Ferronato, C.; Orlando, J. J.; Tyndall, G. S. Rate and Mechanism of the Reactions of OH and Cl with 2-methyl-3-buten-2-ol. *J. Geophys. Res. - Atm.* **1998**, *103*, 25579–25586.
- (9) Paulson, S. E.; Seinfeld, J. H. Development and Evaluation of a Photooxidation Mechanism for Isoprene. *J. Geophys. Res.* **1992**, *97*, 20703–20715.
- (10) Carter, W. P. L.; Atkinson, R. Development and Evaluation of a Detailed Mechanism for the Atmospheric Reactions of Isoprene and NO_x . *Int. J. Chem. Kinet.* **1996**, *28*, 497–530.
- (11) Tuazon, E. C.; Atkinson, R. A Product Study of the Gas-Phase Reaction of Methyl Vinyl Ketone with the OH Radical in the Presence of NO_x . *Int. J. Chem. Kinet.* **1989**, *21*, 1141–1152.

- (12) Nowakowski, D. J.; Bridgwater, A. V.; Elliott, D. C.; Meier, D.; de Wild, P. Lignin Fast Pyrolysis: Results From an International Collaboration. *J. Anal. Appl. Pyrolysis* **2010**, *88*, 53–72.
- (13) Butkovskaya, N. I.; Povesle, N.; Kukui, A.; Le Bras, G. Mechanism of the OH-Initiated Oxidation of Glycolaldehyde Over the Temperature Range 233–296 K. *J. Phys. Chem. A* **2006**, *110*, 13492–13499.
- (14) Calvert, J. G.; Atkinson, R.; Kerr, J. A.; Madronich, S.; Moortgat, G. K.; Wallington, T. J.; Yarwood, G. *The Mechanisms of Atmospheric Oxidation of the Alkenes*; Oxford Univ. Press, 2000.
- (15) Baker, J.; Arey, J.; Atkinson, R. Formation and Reaction of Hydroxycarbonyls From the Reaction of OH Radicals with 1,3-Butadiene and Isoprene. *Environ. Sci. Technol.* **2005**, *39*, 4091–4099.
- (16) Ervens, B.; Carlton, A. G.; Turpin, B. J.; Altieri, K. E.; Kreidenweis, S. M.; Feingold, G. Secondary Organic Aerosol Yields from Cloud-Processing of Isoprene Oxidation Products. *Geophys. Res. Lett.* **2008**, *35*, L02816–L02821.
- (17) Ervens, B.; Volkamer, R. Glyoxal Processing by Aerosol Multiphase Chemistry: Towards a Kinetic Modeling Framework of Secondary Organic Aerosol Formation in Aqueous Particles. *Atmos. Chem. Phys.* **2010**, *10*, 8219–8244.
- (18) Fu, T.-M.; Jacob, D. J.; Wittrock, F.; Burrows, J. P.; Vrekoussis, M.; Henze, D. K. Global Budgets of Atmospheric Glyoxal and Methylglyoxal, and Implications for Formation of Secondary Organic Aerosols. *J. Geophys. Res.* **2008**, *113*, D15303–D15320.
- (19) Washenfelder, R. A.; Young, C. J.; Brown, S. S.; Angevine, W. M.; Atlas, E. L.; Blake, D. R.; Bon, D. M.; Cubison, M. J.; de Gouw, J. A.; Dusanter, S.; et al. The Glyoxal Budget and its Contribution to Organic Aerosol for Los Angeles, California, During CalNex 2010. *J. Geophys. Res.* **2011**, *116*, D00V02–D00V19.
- (20) Nguyen, T. L.; McCarthy, M. C.; Stanton, J. F. Relatively Selective Production of the Simplest Criegee Intermediate in a CH₄/O₂ Electric Discharge: Kinetic Analysis of a Plausible Mechanism. *J. Phys. Chem. A* **2015**, *119*, 7197–7208.
- (21) Friedrichs, G.; Colberg, M.; Dammeier, J.; Bentz, T.; Olzmann, M. HCO Formation In The Thermal Unimolecular Decomposition Of Glyoxal: Rotational And Weak Collision Effects. *Phys. Chem. Chem. Phys.* **2008**, *10*, 6520–6533.
- (22) Vasilou, A. K.; Piech, K. M.; Reed, B.; Zhang, X.; Nimlos, M. R.; Ahmed, M.; Golan, A.; Kostko, O.; Osborn, D. L.; Urness, K. N.; et al. Thermal Decomposition of CH₃CHO Studied by Matrix Infrared Spectroscopy and Photoionization Mass Spectroscopy. *J. Chem. Phys.* **2012**, *137*, 164308.
- (23) Ormond, T. K.; Scheer, A. M.; Nimlos, M. R.; Robichaud, D. J.; Daily, J. W.; Stanton, J. F.; Ellison, G. B. Polarized Matrix Infrared Spectra of Cyclopentadienone: Observations, Calculations, and Assignment for an Important Intermediate in Combustion and Biomass Pyrolysis. *J. Phys. Chem. A* **2014**, *118*, 708–718.
- (24) Ormond, T. K.; Scheer, A. M.; Nimlos, M. R.; Robichaud, D. J.; Troy, T. P.; Ahmed, M.; Daily, J. W.; Stanton, J. F.; Ellison, G. B.; Nguyen, T. L. Pyrolysis of Cyclopentadienone: Mechanistic Insights From a Direct Measurement of Product Branching Ratios. *J. Phys. Chem. A* **2015**, *119*, 7222–7234.
- (25) Porterfield, J. P.; Nguyen, T. L.; Baraban, J. H.; Buckingham, G. T.; Troy, T. P.; Kostko, O.; Ahmed, M.; Stanton, J. F.; Daily, J. W.; Ellison, G. B. Isomerization and Fragmentation of Cyclohexanone in a Heated Micro-Reactor. *J. Phys. Chem. A* **2015**, *119*, 12635–12647.
- (26) Guan, Q.; Urness, K. N.; Ormond, T. K.; David, D. E.; Ellison, G. B.; Daily, J. W. The Properties of a Micro-Reactor for the Study of the Unimolecular Decomposition of Large Molecules. *Int. Rev. Phys. Chem.* **2014**, *33*, 447–487.
- (27) Vasilou, A.; Piech, K. M.; Zhang, X.; Nimlos, M. R.; Ahmed, M.; Golan, A.; Kostko, O.; Osborn, D. L.; Daily, J. W.; Stanton, J. F.; Ellison, G. B.; et al. The Products of the Thermal Decomposition of CH₃CHO. *J. Chem. Phys.* **2011**, *135*, 14306–14311.
- (28) Crocker, L. S. *Thermochemical Investigation Of Carbonyl Compounds By Reaction Calorimetry*. Ph.D. Thesis, Yale University, 1989.
- (29) Wiberg, K. B.; Squires, R. R. Microprocessor-Controlled System For Precise Measurement Of Temperature-Changes - Determination Of The Enthalpies Of Hydrolysis Of Some Polyoxygenated Hydrocarbons. *J. Chem. Thermodyn.* **1979**, *11*, 773–786.
- (30) Martin, E. J. *Investigations of Structure-Energy Relationships by Reaction Calorimetry*. Ph.D. Thesis, Yale University, 1984.
- (31) Morgan, K. M.; Ellis, J. A.; Lee, J.; Fulton, A.; Wilson, S. L.; Dupart, P. S.; Dastoori, R. Thermochemical Studies of Epoxides and Related Compounds. *J. Org. Chem.* **2013**, *78*, 4303–4311.
- (32) Sunner, S.; Wadsö, I. On the Design and Efficiency of Isothermal Reaction Calorimeters. *Acta Chem. Scand.* **1959**, *13*, 97–108.
- (33) Nakaji, D. Y. An ab initio Study of the Effects of Hetero-Substitution on π -Interactions, and, Calorimetry of Nitrogen Containing Heterocycles. Ph.D. Thesis, Yale University, 1992.
- (34) Wiberg, K. B.; Crocker, L. S.; Morgan, K. M. Thermochemical Studies of Carbonyl-Compounds. 5. Enthalpies of Reduction of Carbonyl Groups. *J. Am. Chem. Soc.* **1991**, *113*, 3447–3450.
- (35) Rossini, F. D. Assignment of Uncertainties to Thermochemical Data. In *Experimental Thermochemistry*; Rossini, F. D., Ed.; Interscience: New York City, 1956; pp 297.
- (36) Stanton, J. F.; Gauss, J.; Harding, M. E.; Szalay, P. G. *CFOUR, Coupled-Cluster Techniques for Computational Chemistry*, <http://www.cfour.de>, (2015), with contributions from A.A. Auer, R. J. Bartlett, U. Benedikt, C. Berger, D. E. Bernholdt, Y. J. Bomble, L. Cheng, O. Christiansen, M. Heckert, O. Heun, et al., and the integral packages MOLECULE (J. Almlöf and P. R. Taylor), PROPS (P. R. Taylor), ABACUS (T. Helgaker, H. J. Aa. Jensen, P. Jørgensen, and J. Olsen), and ECP routines by A. V. Mitin and C. van Wüllen.
- (37) Ochterski, J. W.; Petersson, G. A.; Montgomery, J. A. A Complete Basis Set Model Chemistry. 5. Extensions to Six or More Heavy Atoms. *J. Chem. Phys.* **1996**, *104*, 2598–2619.
- (38) Frisch, M. J.; Trucks, G. W.; Schlegel, H. B.; Scuseria, G. E.; Robb, M. A.; Cheeseman, J. R.; Montgomery, J. A., Jr.; Vreven, T.; Kudin, K. N.; Burant, J. C.; et al. *Gaussian 03*; Gaussian, Inc: Wallingford, CT, 2003.
- (39) Hehre, W. J. *Spartan 08*; Wavefunction, Inc, 2009.
- (40) Marstokk, K.-M.; Møllendal, H. Microwave-Spectra Of Isotopic Glycolaldehydes, Substitution Structure, Intramolecular Hydrogen-Bond And Dipole-Moment. *J. Mol. Struct.* **1973**, *16*, 259–270.
- (41) Carroll, P. B.; McGuire, B. A.; Zaleski, D. P.; Neill, J. L.; Pate, B. H.; Weaver, S. L. W. The Pure Rotational Spectrum of Glycolaldehyde Isotopologues Observed in Natural Abundance. *J. Mol. Spectrosc.* **2013**, *284*, 21–28.
- (42) Carroll, P. B.; Drouin, B. J.; Weaver, S. L. W. The Submillimeter Spectrum of Glycolaldehyde. *Astrophys. J.* **2010**, *723*, 845–849.
- (43) Bouchez, A.; Margules, L.; Motiyenko, R. A.; Guillemin, J. C.; Walters, A.; Bottinelli, S.; Ceccarelli, C.; Kahane, C. The Submillimeter Spectrum of Deuterated Glycolaldehydes. *Astron. Astrophys.* **2012**, *540*, A51–A57.
- (44) Haykal, I.; Motiyenko, R. A.; Margules, L.; Huet, T. R. Millimeter And Submillimeter Wave Spectra of ¹³C-Glycolaldehydes. *Astron. Astrophys.* **2013**, *549*, A96–A112.
- (45) Gordy, W.; Cook, R. L. *Microwave Molecular Spectra*; Interscience Publishers: New York City, 1970.
- (46) Costain, C. C. Determination of Molecular Structures from Ground State Rotational Constants. *J. Chem. Phys.* **1958**, *29*, 864–874.
- (47) Kraitchman, J. Determination of Molecular Structure From Microwave Spectroscopic Data. *Am. J. Phys.* **1953**, *21*, 17–24.
- (48) Kroto, H. W. *Molecular Rotation Spectra*; John Wiley & Sons: London, U.K, 1975; pp 156–163.
- (49) Afeefy, H. Y.; Liebman, J. F.; Stein, S. E. Neutral Thermochemical Data. In *NIST Chemistry WebBook*; NIST Standard Reference Database Number 69; National Institute of Standards and Technology: Gaithersburg, MD. <http://webbook.nist.gov>, retrieved November 30, 2015.
- (50) Michelsen, H.; Klabe, P. Spectroscopic Studies of Glycolaldehyde. *J. Mol. Struct.* **1969**, *4*, 293–302.

- (51) Kobayashi, Y.; Takahara, H.; Takahashi, H.; Higasi, K. Infrared and Raman Studies of Structure of Crystalline Glycolaldehyde. *J. Mol. Struct.* **1976**, *32*, 235–246.
- (52) Mohacek-Grosov, V.; Prugovecki, B.; Prugovecki, S.; Strukan, N. Glycolaldehyde Dimer in the Stable Crystal Phase has Axial OH Groups: Raman, Infrared and X-ray Data Analysis. *J. Mol. Struct.* **2013**, *1047*, 209–215.
- (53) Wiberg, K. B.; Waldron, R. F. Lactones. 2. Enthalpies of Hydrolysis, Reduction, and Formation of the C₄-C₁₃ Monocyclic Lactones. Strain Energies and Conformations. *J. Am. Chem. Soc.* **1991**, *113*, 7697–7705.
- (54) Wiberg, K. B. Accuracy of Calculations of Heats of Reduction/Hydrogenation: Application to Some Small Ring Systems. *J. Org. Chem.* **2012**, *77*, 10393–10398.
- (55) Cox, J. D.; Pilcher, G. *Thermochemistry of Organic and Organometallic Compounds*; Academic Press: New York City, 1970.
- (56) Reid, R. C.; Prausnitz, J. M.; Sherwood, T. K. *The Properties of Gases and Liquids*; McGraw-Hill Book Company: New York City, 1977.
- (57) Acree, W., Jr.; Chickos, J. S. Phase Transition Enthalpy Measurements of Organic and Organometallic Compounds. Sublimation, Vaporization and Fusion Enthalpies From 1880 to 2010. *J. Phys. Chem. Ref. Data* **2010**, *39*, 043101–044043.
- (58) Petitjean, M.; Reyes-Perez, E.; Perez, D.; Mirabel, P.; Le Calve, S. Vapor Pressure Measurements of Hydroxyacetaldehyde and Hydroxyacetone in the Temperature Range (273 to 356) K. *J. Chem. Eng. Data* **2010**, *55*, 852–855.
- (59) Pedley, J. B.; Naylor, R. D.; Kirby, S. P. *Thermochemistry of Organic Compounds*, 2 ed.; Chapman and Hall: New York, 1986.
- (60) Cramer, C. J.; Truhlar, D. G. Quantum-Chemical Conformational-Analysis of 1,2-Ethandiol - Correlation and Solvation Effects on the Tendency to Form Internal Hydrogen-Bonds in The Gas-Phase and in Aqueous-Solution. *J. Am. Chem. Soc.* **1994**, *116*, 3892–3900.
- (61) Bouchoux, G.; Penaud-Berruyer, F.; Bertrand, W. Structure, Thermochemistry and Reactivity of Protonated Glycolaldehyde. *Eur. Mass Spectrom.* **2001**, *7*, 351–357.
- (62) Espinosa-Garcia, J.; Dóbé, S. Theoretical Enthalpies of Formation for Atmospheric Hydroxycarbonyls. *J. Mol. Struct.: THEOCHEM* **2005**, *713*, 119–125.
- (63) Ptasinska, S.; Denifl, S.; Scheier, P.; Märk, T. D. Electron Impact Ionization of Glycolaldehyde. *Int. J. Mass Spectrom.* **2005**, *243*, 171–176.
- (64) Goddard, W. A., III; Harding, L. B. Description of Chemical Bonding from Ab initio Calculations. *Annu. Rev. Phys. Chem.* **1978**, *29*, 363–396.
- (65) Blanksby, S. J.; Ellison, G. B. Bond Dissociation Energies of Organic Molecules. *Acc. Chem. Res.* **2003**, *36*, 255–263.
- (66) Vasiliou, A. K.; Kim, J. H.; Ormond, T. K.; Piech, K. M.; Urness, K. N.; Scheer, A. M.; Robichaud, D. J.; Mukarakate, C.; Nimlos, M. R.; Daily, J. W.; et al. Biomass Pyrolysis: Thermal Decomposition Mechanisms of Furfural and Benzaldehyde. *J. Chem. Phys.* **2013**, *139*, 104310–104321.
- (67) Schwell, M.; Gaie-Levrel, F.; Bénilan, Y.; Gazeau, M.-C.; Fray, N.; Saul, G.; Champion, N.; Leach, S.; Guillemin, J.-C. VUV Spectroscopy and Photochemistry of Five Interstellar and Putative Prebiotic Molecules. In *EAS Publication Series*; Stehle, C., Joblin, C., d'Hendecourt, L., Eds., **2012**; Vol. 58, pp 301–306.10.1051/eas/1258050
- (68) McLafferty, F. W.; McAdoo, D. J.; Smith, J. S.; Kornfeld, R. Enolic C₃H₆O^{•+} Ion Formed from Aliphatic Ketones. *J. Am. Chem. Soc.* **1971**, *93*, 3720–3730.
- (69) Smith, I. W. M.; Ravishankara, A. R. Role of hydrogen-bonded intermediates in the bimolecular reactions of the hydroxyl radical. *J. Phys. Chem. A* **2002**, *106*, 4798–4807.
- (70) Ceponkus, J.; Chin, W.; Chevalier, M.; Broquier, M.; Limongi, A.; Crepin, C. Infrared Study of Glycolaldehyde Isolated in Para Hydrogen Matrix. *J. Chem. Phys.* **2010**, *133*, 094502–094509.
- (71) Shimanouchi, T. *Tables of Vibrational Frequencies*, Consolidated Vol. I; NSRDS-NBS 39, 1972.
- (72) The six modes of formaldehyde as observed in an Ar matrix are: ν_1 (a₁, CH₂ sym st) = 2798 cm⁻¹, ν_2 (a₁, CO st) = 1742 cm⁻¹, ν_3 (a₁, CH₂ scis) = 1499 cm⁻¹, ν_4 (b₁, CH₂ umbrella) = 1169 cm⁻¹, ν_5 (b₂, CH₂ a-st) = 2864 cm⁻¹, ν_6 (b₂, CH₂ rock) = 1245 cm⁻¹.
- (73) Shimanouchi, T. Tables of Molecular Vibrational Frequencies. Consolidated Volume II. *J. Phys. Chem. Ref. Data* **1977**, *6*, 993–1102.
- (74) Nelander, B. A Matrix-Isolation Study of The Water Formaldehyde Complex - The Far-Infrared Region. *Chem. Phys.* **1992**, *159*, 281–287.
- (75) Garcia-Moreno, I.; Moore, C. B. Spectroscopy of Methylene - Einstein Coefficients for CH₂ (B ¹b₁ — A ¹a₁) Transitions. *J. Chem. Phys.* **1993**, *99*, 6429–6435 This paper reports the gas-phase IR bands of ketene. By use of an authentic sample of CH₂=C=O, we observed ketene modes in an Ar matrix. We find a₁ bands (ν_1 = 3062.9 cm⁻¹, ν_2 = 2142.3 cm⁻¹, ν_3 = 1382.3 cm⁻¹, ν_4 = 1114 cm⁻¹); b₁ modes (ν_5 = 598 cm⁻¹, ν_6 = 524.3 cm⁻¹); b₂ fundamentals (ν_7 = 3158 cm⁻¹, ν_8 = 973.1 cm⁻¹, ν_9 is below detector wavelength range).
- (76) Bühl, M.; Kramme, R.; Martin, H. D.; Mayer, B.; Nowack, G. Chromophoric Systems. 1. Conformation and Absorption of Light in Hexa-1,5-Diene-3,4-Dione (Divinylglyoxal). *Chem. Ber.* **1991**, *124*, 821–826.
- (77) Engdahl, A.; Nelander, B. Infrared-spectrum of cis-glyoxal. *Chem. Phys. Lett.* **1988**, *148*, 264–268.
- (78) Leroi, G. E.; Ewing, G. E.; Pimentel, G. C. Infrared Spectra of Carbon Monoxide in Argon Matrix. *J. Chem. Phys.* **1964**, *40*, 2298–2303.
- (79) Hartley, D. B. Chemiluminescent Recombination of Formyl Radicals. *Chem. Commun.* **1967**, 1281–1282.
- (80) Fletcher, R. A.; Pilcher, G. Measurements of Heats of Combustion by Flame Calorimetry Part 6. Formaldehyde, Glyoxal. *Trans. Faraday Soc.* **1970**, *66*, 794–799.
- (81) Moore, C. E. *Atomic Energy Levels*; National Bureau of Standards: Washington, DC, 1971; NSRDS-NBS 35, Vol. 1.
- (82) Wiedmann, R. T.; Tonkyn, R. G.; White, M. G.; Wang, K. H.; McKoy, V. Rotationally Resolved Threshold Photoelectron-Spectra of OH and OD. *J. Chem. Phys.* **1992**, *97*, 768–772.
- (83) Evans, M.; Ng, C. Y. Rotationally Resolved Pulsed Field Ionization Photoelectron Study of CO⁺(X ²Σ⁺, v⁺ = 0–42) in the Energy Range of 13.98–21.92 eV. *J. Chem. Phys.* **1999**, *111*, 8879–8892.
- (84) Schulenburg, A. M.; Meisinger, M.; Radi, P. P.; Merkt, F. The Formaldehyde Cation: Rovibrational Energy Level Structure and Coriolis Interaction Near the Adiabatic Ionization Threshold. *J. Mol. Spectrosc.* **2008**, *250*, 44–50.
- (85) Tonkyn, R. G.; Winniczek, J. W.; White, M. G. Rotationally Resolved Photoionization of O₂⁺ Near Threshold. *Chem. Phys. Lett.* **1989**, *164*, 137–142.
- (86) Niu, B. H.; Bai, Y.; Shirley, D. A. High-Resolution Photoelectron-Spectroscopy and Femtosecond Intramolecular Dynamics of CH₂CO⁺ and CD₂CO⁺. *J. Chem. Phys.* **1993**, *99*, 2520–2532.
- (87) Taatjes, C. A.; Hansen, N.; McIlroy, A.; Miller, J. A.; Senosiain, J. P.; Klippenstein, S. J.; Qi, F.; Sheng, L. S.; Zhang, Y. W.; Cool, T. A.; et al. Enols are Common Intermediates in Hydrocarbon Oxidation. *Science* **2005**, *308*, 1887–1889.
- (88) Knowles, D. J.; Nicholson, A. J. C. Ionization Energies of Formic and Acetic-Acid Monomers. *J. Chem. Phys.* **1974**, *60*, 1180–1181.
- (89) Mucha, M.; Mielke, Z. Complexes of Atmospheric Alpha-Dicarbonyls with Water: FTIR Matrix Isolation and Theoretical Study. *J. Phys. Chem. A* **2007**, *111*, 2398–2406.